

Research paper

## Stochastic resonance in dissipative drift motion



Ricardo S. Oyarzabal<sup>a,b</sup>, José D. Szezech Jr<sup>a,c</sup>, Antonio M. Batista<sup>a,c,d,e,\*</sup>,  
Jesus M. Seoane<sup>b</sup>, Miguel A.F. Sanjuán<sup>b,f</sup>

<sup>a</sup> Pós-Graduação em Ciências, Universidade Estadual de Ponta Grossa, 84030-900, Ponta Grossa, PR, Brazil

<sup>b</sup> Departamento de Física, Universidad Rey Juan Carlos, Tulipán s/n, 28933 Móstoles, Madrid, Spain

<sup>c</sup> Departamento de Matemática e Estatística, Universidade Estadual de Ponta Grossa, 84030-900, Ponta Grossa, PR, Brazil

<sup>d</sup> Instituto de Física, Universidade de São Paulo, 05315-970, São Paulo, SP, Brazil

<sup>e</sup> Institute for Complex Systems and Mathematical Biology, University of Aberdeen, Scotland, UK

<sup>f</sup> Institute for Physical Science and Technology, University of Maryland, College Park, Maryland 20742, USA

### ARTICLE INFO

#### Article history:

Received 13 September 2016

Revised 14 April 2017

Accepted 22 May 2017

Available online 23 May 2017

#### Keywords:

Noise

Stochastic resonance

Drift motion

### ABSTRACT

We study a simple model of drift waves that describes the particle transport in magnetised plasmas. In particular, we focus our attention on the effects of noise on a dissipative drift wave model. In the noiseless case, the relationship between the escape time and the damping term obeys a power-law scaling. In this work, we show that peaks in the escape time are enhanced for certain values of the noise intensity, when noise is added in the dissipative drift motion. This enhancement occurs in the situation where stochastic resonance (SR) appears. We also observe that the noise produces significant alterations to the escape time distribution. This way, we expect this work to be useful for a better understanding of drift wave models in the presence of noise, since noise is a natural ingredient in the environment of this kind of physical problems.

© 2017 Elsevier B.V. All rights reserved.

## 1. Introduction

Drift waves can appear in magnetically confined plasmas [1]. They have a frequency lower than the frequencies related to magnetohydrodynamic waves, and they have been widely investigated in anomalous diffusion across magnetic fields [2], mainly in drift wave turbulence in toroidal plasmas [3,4]. An experiment in a plasma where collisional drift waves were identified, has been carried out in [5]. Besides, a relationship between collisional drift waves and enhanced plasma transport was observed. A theoretical description of drift waves has been proposed by Horton [6], where conditions on the drift wave for stochasticity and the validity of the diffusion approximation have been proposed.

Drift waves for a large aspect ratio tokamak can be described by two-wave Hamiltonian model. In the present work, we have included modifications in the two-wave Hamiltonian model, which we describe now. The two-wave Hamiltonian model has been considered to describe particle transport [2]. This model can exhibit island chains in phase space, as well as chaotic behaviour [7]. The effect of dissipation was previously studied in Ref. [8]. In this work, we modify the model including not only a dissipative term, but also a noisy term aiming at studying the escape times in this system. In spite of the importance of the effect of noise in the dynamics, this has been scarcely considered in previous works on the two-wave Hamiltonian model.

\* Corresponding author.

E-mail address: [antoniomarcosbatista@gmail.com](mailto:antoniomarcosbatista@gmail.com) (A.M. Batista).

Certainly, the effects of noise on dynamical systems are relevant in science and engineering [9]. Precisely, one of the effects of noise is the well-known phenomenon of stochastic resonance (SR). It mainly consists in the appearance of a cooperative effect between the internal mechanism and the external forcing [10,11], and as a consequence SR improves a system performance measure. SR has been observed and studied in many systems, leading to important experimental and theoretical results [12]. Park and Lai [13] showed that a common feature of SR is the high sensitivity to the variation of noise. Gluckman and collaborators [14] experimentally demonstrated the existence of SR in neuronal networks from the mammalian brain. The SR has been also studied in a large variety of systems, such as climatic change [15], biological cells [16], and more recently in problems of periodic potentials [17] and anharmonic oscillators with coexisting attractors [18].

The purpose of this article is to investigate the effects of noise on the escape time in the dissipative drift motion. In our context, noise can represent the collision effect between particles [19]. The escape time features in Hamiltonian drift waves were studied in Refs. [20–23]. Escape time in a dissipative drift wave model without noise was already analysed by Oyarzabal et al. [8], where a power-law in the escape time as a function of the dissipation parameter was found. The main conclusions of this work are the presence of SR and the extreme sensitivity of the escape time, as a function of the noise intensity. Therefore, the escape times are large in this SR situation, and as a result particles are trapped for a long time.

The paper is organised as follows. In Section 2, we briefly describe the drift wave model and we introduce a noise term in the dissipative model. In Section 3, we verify some SR characteristics in the dissipative drift motion with noise, where we observe that the escape time can be maximal when the noise intensity reaches a finite level. Finally, the conclusions are presented in Section 4.

## 2. Effect of noise in the dissipative drift motion

Here we analyse a model of drift waves that describes the transport of particles in a magnetically confined plasma. In a magnetised plasma the electrostatic wave propagation is in the poloidal direction and the drift velocity of the guiding centers is given by [6]

$$\vec{v} = \frac{\vec{E} \times \vec{B}}{B^2}, \quad (1)$$

with electric field  $\vec{E} = -\nabla\phi$ , constant toroidal magnetic field  $\vec{B} = B_0\hat{e}_z$ , and electrostatic potential

$$\phi(x, y, t) = \phi_0(x) + \sum_{i=1}^N A_i \sin(k_{xi}x) \cos(k_{yi}y - \omega_i t + \beta_i), \quad (2)$$

where  $A_i$  is the amplitude of the  $i$ th wave,  $k_{xi}$  and  $k_{yi}$  are the wavenumbers in the  $x$  direction (radial coordinate) and  $y$  direction (poloidal coordinate), respectively. Furthermore,  $\omega_i$  is the angular frequency,  $\beta_i$  is the phase,  $N$  is the number of electrostatic drift waves propagating in the poloidal direction  $y$ , and  $\phi_0(x)$  is the equilibrium electrostatic potential that depends on the radial electric field profile. In our case, we have used a uniform electric field  $\phi_0(x) = ax$ . Eq. (2) is a simple nonlinear description based on computer simulations and analytical studies reported by Horton in drift waves [24]. With regard to phases, Bénisti and Escande [25] considered initial random phases in a set of electrostatic waves to study diffusion properties of the standard map, for instance the case in the beam-plasma instability. The influence of the phases on the motion of a particle in the field of many waves was investigated by Elskens [26]. In our simulations, we consider the phases with values equal to zero according to work about drift waves and transport by Horton [2]. Batista et al. [27] also used phases equal to zero in a nonlinear three-mode interaction model to analyse the occurrence of drift wave turbulence driven by pressure gradient in the edge plasma of a tokamak [28]. In our work, for  $\beta_i = 0$ , the model exhibits a rich dynamical behaviour with chaotic and periodic dynamics, which can be used to describe drift wave driven transport.

Substituting the electrostatic potential into the Hamiltonian  $H(x, y, t) = \phi/B_0$  and introducing the variables

$$\begin{aligned} x' &= \frac{x}{r_0}, y' = \frac{y}{r_0}, a' = \frac{a}{E_0}, t' = \frac{t}{t_0}, \\ \omega' &= \omega_i t_0, A'_i = \frac{A_i}{E_0 r_0}, \vec{k}'_i = \vec{k}_i r_0, \end{aligned} \quad (3)$$

we obtain the dimensionless Hamiltonian [6]

$$H(x, y, t) = ax + \sum_{i=1}^N A_i \sin(k_{xi}x) \cos(k_{yi}y - \omega_i t). \quad (4)$$

This system is integrable and exhibits stable orbits when  $N = 1$ . For  $N > 1$  the system is integrable if the phase velocities are the same, and it is not integrable if at least one phase velocity is different. In the nonintegrable case the system exhibits chaotic dynamics.

We find the equations of motion for the drift caused by two waves from the dimensionless Hamiltonian. In these equations, we have introduced dissipation as in Ref. [8] and a noise term. Dissipation is the result of many processes that can be due to ion viscosity, ion-ion or ion-neutral collisions, ion Landau-damping, and coupling to damped modes such as ion-acoustic waves [29]. Kabantsev et al. [30] verified that chaotic collisional neoclassical transport causes enhanced dissipation

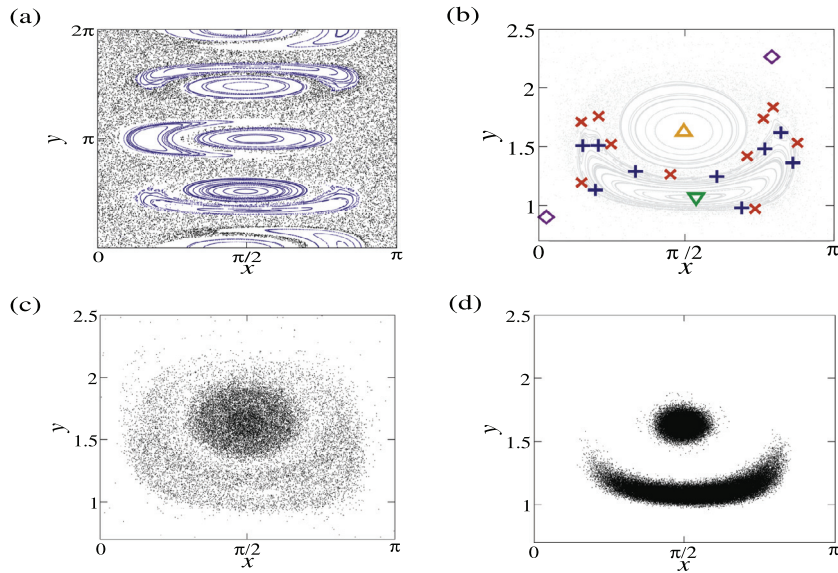


**Fig. 1.** The figure shows the Poincaré section for a different set of parameters of the two drift waves model:  $A_1 = 1$ ,  $A_2 = 0.1$ ,  $k_{x1} = 1$ ,  $k_{x2} = \sqrt{3}$ ,  $k_{y1} = 1$ ,  $k_{y2} = 0.5$ , and  $u = 1.5$ , for (a)  $\sigma = 0$  and  $\mu = 0$ , (b)  $\sigma = 0$  and  $\mu = 10^{-3}$ , (c)  $\sigma = 10^{-2}$  and  $\mu = 0$ , and (d)  $\sigma = 10^{-2}$  and  $\mu = 10^{-3}$ .

in parametric drift wave decay. As what concerns the noise, we have considered a white noise distribution [31]. According to the previous point, the evolution equations of our model for two drift waves with dissipation and noise are given by

$$\begin{aligned} \frac{dx}{dt} &= A_1 k_{y1} \sin(k_{x1}x) \sin(k_{y1}y) \\ &\quad + A_2 k_{y2} \sin(k_{x2}x) \sin(k_{y2}(y - ut)) - \mu x + \sigma \xi_x \\ \frac{dy}{dt} &= A_1 k_{x1} \cos(k_{x1}x) \cos(k_{y1}y) \\ &\quad + A_2 k_{x2} \cos(k_{x2}x) \cos(k_{y2}(y - ut)) - \mu y + \sigma \xi_y, \end{aligned} \quad (5)$$

where  $x$  and  $y$  vary from  $-\infty$  to  $+\infty$ ,  $u = |\frac{\omega_2}{k_{y2}} - \frac{\omega_1}{k_{y1}}|$  is the phase velocity difference between the two waves,  $\mu$  is the dissipation parameter,  $\sigma$  is the noise intensity,  $\xi_x$  and  $\xi_y$  are the random fluctuations. In our numerical simulations we have considered  $A_1 = 1$ ,  $A_2 = 0.1$ ,  $k_{x1} = 1$ ,  $k_{x2} = \sqrt{3}$ ,  $k_{y1} = 1$ ,  $k_{y2} = 0.5$ , and  $u = 1.5$  as in Refs. [7,8]. We also consider  $a = 0$ , and as a result all orbits of the noiseless conservative model are closed and are given in terms of Jacobi elliptic functions [24].

The Poincaré section of the phase space for the noiseless case [32,33], is shown in Fig. 1. The points in the Poincaré section correspond to values from the equations of motion plotted at each time period given by  $2\pi/u$ . In absence of dissipation, the Poincaré section (Fig. 1a) shows island chains (in blue colour), which are immersed in a chaotic sea (in black colour). Fig. 1(b) is a magnification of Fig. 1(a), where the gray points correspond to  $\mu = 0$  (conservative) and the coloured symbols to  $\mu = 10^{-3}$  (dissipative). A small amount of dissipation is enough for the system to present a dynamics dominated by the appearance and disappearance of periodic attractors. In Fig. 1(b) there are two period-1 attractors, one denoted by an orange triangle and another by a green triangle. We have also one period-2 attractor denoted by violet diamonds, one period-9 attractor represented by blue pluses, and one period-10 attractor identified by red crosses. Figs. 1(c) and (d) show that noise is able to destroy not only the islands chains and the chaotic sea in the conservative case, but also the attractors in the dissipative drift wave model.

We plot, in Fig. 2(a) and (b), single trajectories of the model for different values of the noise intensity  $\sigma$  with values of the dissipation  $\mu$  equal to 0 and  $10^{-3}$ , respectively. In Fig. 2(a), we observe that the noise intensity helps the particles to escape from the confinement region. We also notice that the worst performance for the escapes takes place for the noiseless conservative case, which means that this initial condition does not escape from the confinement region, trapped in an orbit. In addition, the noiseless conservative system can exhibit either Kolmogorov-Arnold-Moser (KAM) islands and chaotic regions in the phase space. The dissipation destroys not only the KAM tori, but also the chaotic region. As a result, the KAM islands originate periodic attractors. Considering dissipation, the noiseless system exhibits attractors, however when noise is added we verify that trajectories can escape depending on the noise intensity. The ability of noise to destroy some attractors has been verified in the literature [34]. According to our numerical precision, we observe the annihilation of very small attractor basins for  $\sigma \approx 10^{-6}$ . The effect of a small noise on an initial condition in the attractor basin is observed in Fig. 2(b). For  $\sigma = 0$ , the trajectory remains in the attractor basin, while for  $\sigma > 0$  the trajectories go outside their basin. We have also verified that there is a relationship between the noise intensity and the escape time.

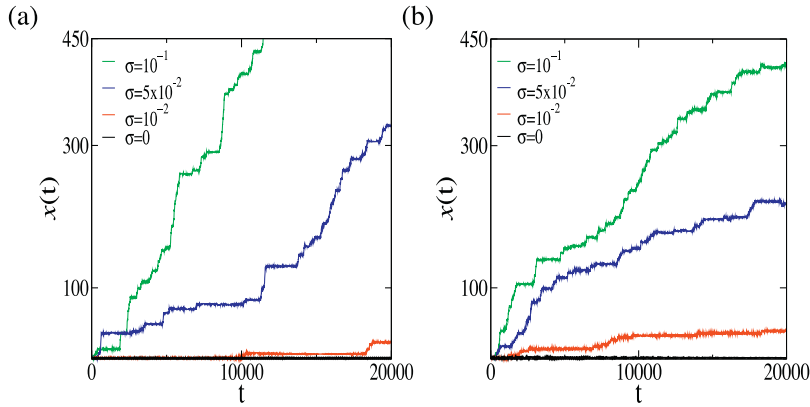


Fig. 2. Trajectories of one initial condition for different values of the noise intensity for (a)  $\mu = 0$  and (b)  $\mu = 10^{-3}$ .

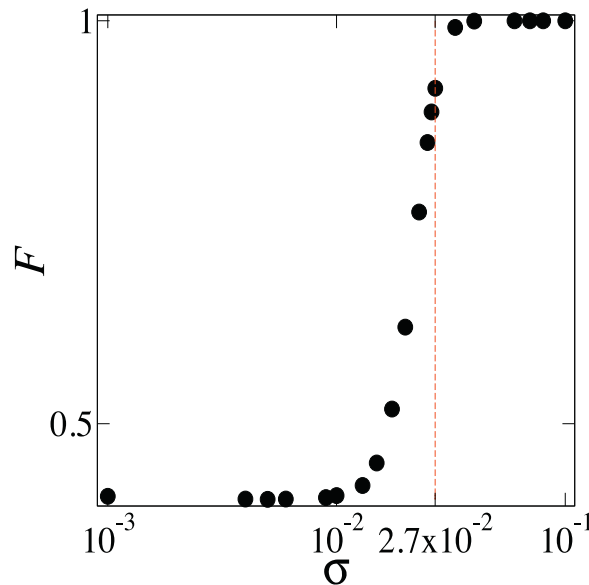


Fig. 3. Fraction of escaped particles from the region  $Q$  varying the noise intensity. The dash line for  $\sigma = 2.7 \times 10^{-2}$  is where the averaged escape time is maximum.

### 3. Stochastic resonance in the dissipative drift model

The SR phenomenon appears when the system is affected by some external noise in a specific situation. In our case, this phenomenon helps the particles to be confined in a region for a very long time. For this reason, our goal here is to study the escape time in a  $\vec{E} \times \vec{B}$  drift motion in presence of noise. The escape time is the time that a particle remains trapped before escaping from an specific region  $Q$ . We call this region  $Q$ , which is the region defined by the domain  $[0, \pi] \times [0.7, 2.5]$ . The domain  $Q$  is chosen according to two criteria: (1) a domain size that includes all periodic attractors observed in Fig. 1(b); (b) the spatial periodicity. There is a repetition of the periodic attractors for coordinates  $x$  and  $y$ , every  $\pi$  and  $\pi/2$ , respectively. For this reason, the big size domain does not include more than once the periodic attractors.

We have calculated the fraction of escaped particles from the defined grid as a function of the noise intensity (Fig. 3). The fraction is given by  $F = N_{esc}/N$ , where  $N_{esc}$  and  $N$  are the number of particles that escape and the total number of particles, respectively. We have verified that in the case  $\mu = 10^{-3}$ , all particles escape ( $F = 1$ ) when  $\sigma$  is approximately greater than  $6 \times 10^{-2}$ . (Fig. 3). The dash line corresponds to the  $\sigma$  value ( $\sigma = 2.7 \times 10^{-2}$ ), where the average escape time is maximum. The particles that escape can go to attractors outside our bounded domain.

In order to attest the behaviour of the escape time with the dissipation and noise parameters, we have computed the average escape time

$$\langle \tau \rangle = \frac{1}{M} \sum_{m=1}^M \tau_m, \tag{6}$$

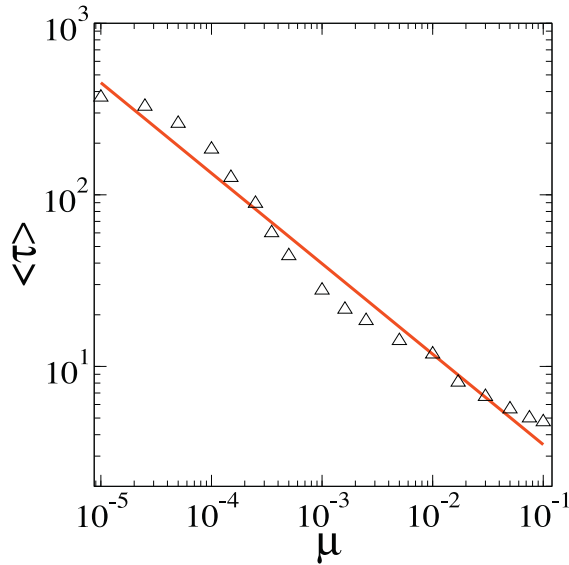


**Fig. 4.** Escape time versus the dissipation parameter. The red solid line is a fit given by  $\langle \tau \rangle = 1.04\mu^{-0.53}$ , where  $2.5 \times 10^5$  initial conditions have been shot. (For interpretation of the references to colour in this figure legend, the reader is referred to the web version of this article.)

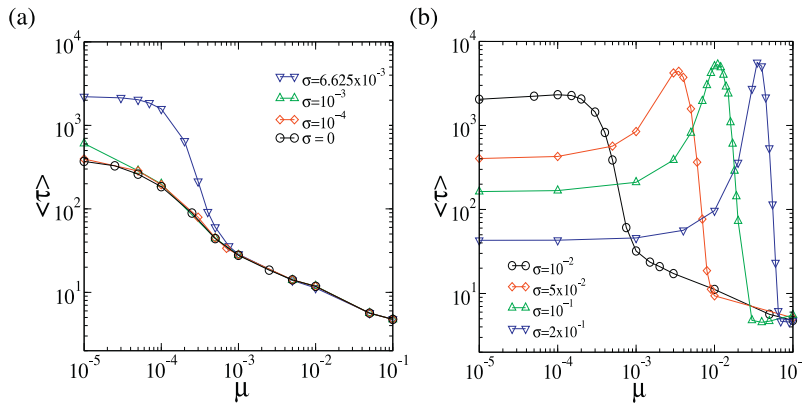


**Fig. 5.** (a) Escape time as a function of the dissipation parameter for noise values  $\sigma = 0, \sigma = 10^{-4}, \sigma = 10^{-3}$  and  $\sigma = 6.625 \times 10^{-3}$ , respectively. We observe the decreasing of the escape time when dissipation becomes large. In (b) we have the escape time as a function of the dissipation parameter for noise values  $\sigma = 10^{-2}, 5 \times 10^{-2}, 10^{-1}, 2 \times 10^{-2}$ , respectively. We observe the onset of the SR phenomenon when noise intensity  $\sigma \approx 6.63 \times 10^{-3}$ .

where  $M$  is the number of initial conditions that escape from the region  $Q$ , previously defined, and  $\tau_m$  is the escape time for every initial condition. Eq. (6) does not diverge ( $M > 0$ ), even for the largest value of the dissipation that we consider in our simulations, because the particles near the borders of the region  $Q$  escape to attractors outside this domain. Notice that, from now on and for our convenience, we simply call  $\tau$  *escape time* instead of “average escape time”. We compute the escape time by shooting  $2.5 \times 10^5$  initial conditions. Fig. 4 shows the dependence of  $\langle \tau \rangle$  with the dissipation parameter for  $\sigma = 0$ . We have verified that the functional relationship between  $\langle \tau \rangle$  and  $\mu$  follows a power-law form, where the fit is given by  $\langle \tau \rangle = 1.04\mu^{-0.53}$  [8]. In absence of noise, it is observed that the escape time decreases insofar the dissipation parameter increases. Moreover, in Fig. 4 we see not only a scaling law, but also an oscillation around the power-law fit. This oscillatory behaviour was also observed in other models by Krawiecki et al. [35], where log-periodic oscillations around the power-law trend of the escape probability from an attractor was observed in chaotic maps close to a crisis.

We study the effects of noise in our model. As in the noiseless case shown previously, we shot  $2.5 \times 10^5$  initial conditions for  $t = 2 \times 10^4$  time units contained in the region  $Q$ . Fig. 5(a) shows the variation of the escape time with the dissipation parameter  $\mu$  for different values of  $\sigma$ , namely  $\sigma = 0, \sigma = 10^{-4}, \sigma = 10^{-3}$  and  $6.625 \times 10^{-3}$ , respectively. An increase in the escape time is observed insofar the value of the noise intensity is increased. At the same time and in the same figure, we see that the escape time decreases as the dissipation increases, reaching a saturation phenomenon when  $\mu = 10^{-3}$ . The curves seem to fit each other for values larger than  $\mu = 10^{-3}$ . It means that there is a saturation in the escape time for large values of the dissipation. We also see in Fig. 5(a) that for noise values close to  $\sigma = 6.63 \times 10^{-3}$  a decrease of the escape time in function of dissipation occurs, and for large values of the dissipation parameter,  $\mu = 10^{-3}$ , the curves are saturated.

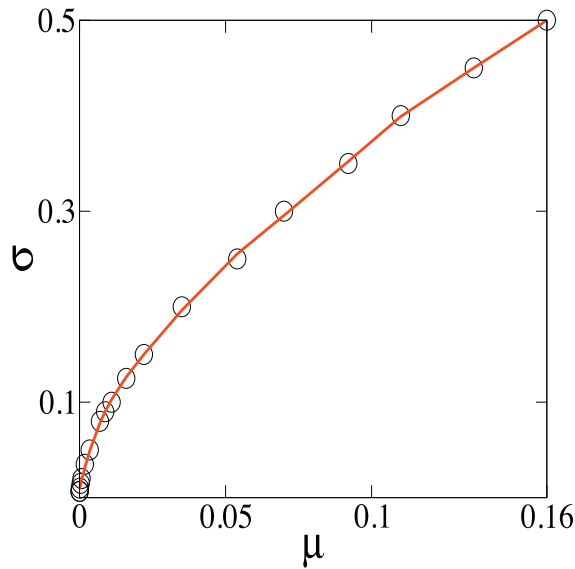


**Fig. 6.** Noise versus dissipation where each circle denotes the values of  $\sigma$  and  $\mu$  when  $\langle \tau \rangle$  is maximum. The red line is the fit given by  $\sigma = \sqrt{2\mu}$ . (For interpretation of the references to colour in this figure legend, the reader is referred to the web version of this article.)

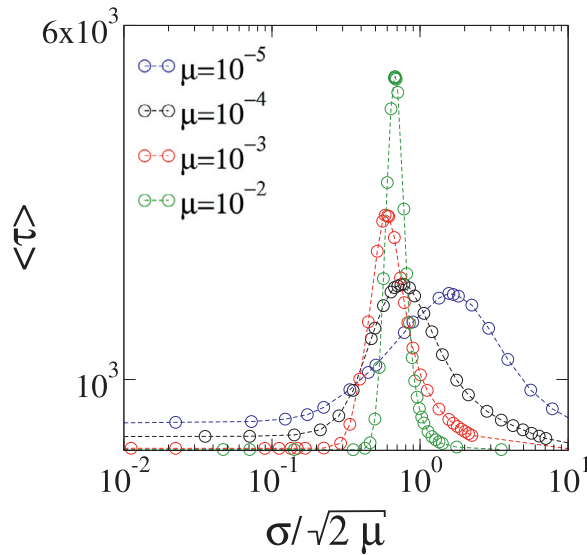


**Fig. 7.** Escape time versus noise intensity for different dissipation parameter values.

We also want to analyse what happens if the noise intensity increases. For this purpose, we have plotted in Fig. 5(b) the escape time  $\langle \tau \rangle$  versus the dissipative parameter  $\mu$  for high values of noise  $\sigma = 10^{-2}$ ,  $5 \times 10^{-2}$ ,  $\sigma = 10^{-1}$ , and  $2 \times 10^{-1}$ . Fig. 5(b) shows that the behaviour of the curves changes for values of noise larger than  $\sigma_c = 6.63 \times 10^{-3}$ . For values of  $\sigma$  larger than  $\sigma_c$ , we uncover a SR phenomenon for which the particles are trapped and they escape from the confined region more slowly than in both the conservative and the dissipative cases. In these cases, we see that certain values of the dissipation and noise terms can improve the confinement of particles. In our simulations, we observe that the escape times increase for these optimal values of  $\sigma$ .

Fig. 6 exhibits the relationship between the noise term and the dissipative term when  $\langle \tau \rangle$  is maximum. The maximum values (circles) correspond to the peaks showed in Fig. 5. As a result, we observe that the curve presents a fit given by  $\sigma = \sqrt{2\mu}$ . This way, the values of the noise intensity and dissipation for the largest escape time can be found by means of the fitted equation.

The fitted equation from the points in Fig. 6 gives us the  $\sigma$  and  $\mu$  values when  $\langle \tau \rangle$  is only maximum. Aiming to analyse the behaviour of  $\langle \tau \rangle$  around the maximum point, we plot  $\langle \tau \rangle$  versus  $\sigma$ . Fig. 7 shows the plot for various values of the dissipation parameter such as  $10^{-5}$ ,  $10^{-4}$ ,  $10^{-3}$ , and  $10^{-2}$ , where the escape time value is computed from a set of  $2.5 \times 10^5$  initial conditions for 20000 time units inside the region  $Q$ . We observe in Fig. 7 that the curve of the escape time as a

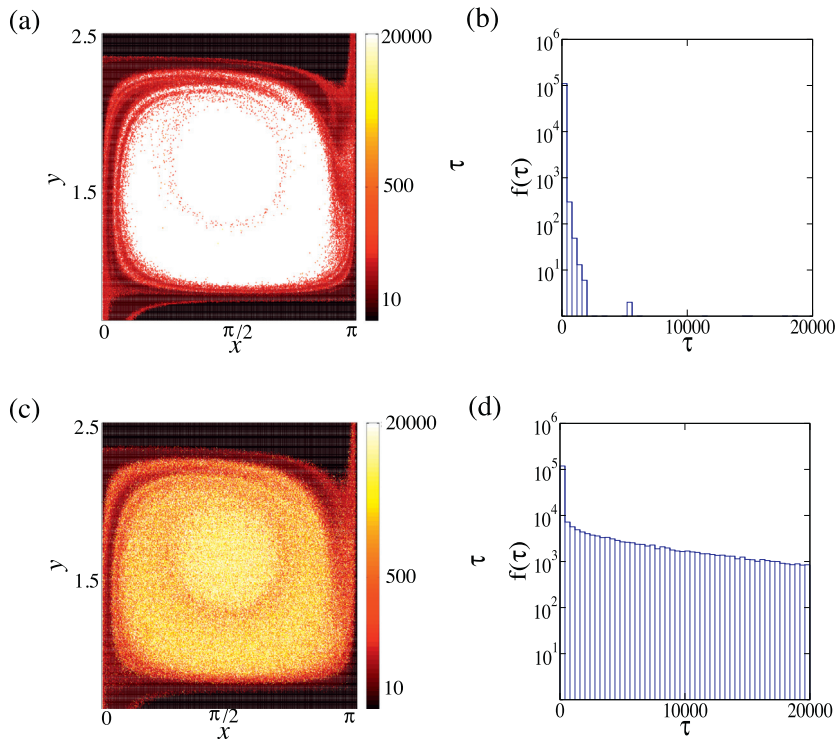


**Fig. 8.** Escape time in colour bar for dissipation parameter and noise intensity, where we consider (a)  $\mu = 10^{-3}$  and  $\sigma = 10^{-2}$ , and (c)  $\mu = 10^{-3}$  and  $\sigma = 2.7 \times 10^{-2}$ . Figures (b) and (d) correspond to the escape time distributions for (a) and (c), respectively.

function of the noise exhibits a maximum value for different values of  $\mu$ . For  $\mu = 10^{-5}$  (blue circles) the curve displays an optimal value of noise amplitude close to  $\sigma = 6.63 \times 10^{-3}$ . According to our results, by increasing the value of  $\mu$  for  $10^{-4}$  (black circles),  $10^{-3}$  (red circles), and  $10^{-2}$  (green circles), we can see that not only the peak changes the position, but also the standard deviation of the escape time distribution decreases. Therefore, through Figs. 5(b) and 7 we can find the  $\sigma$  and  $\mu$  values for which the SR phenomenon happens, namely the largest escape time of particles subjected to two drift waves.

This way, we have detected the SR phenomenon due to the fact that the noise added to the dissipative drift motion produces changes in the behaviour of the escape time. This study provides us new insights on the effects of noise in escaping dynamics of particles, such as in this case in magnetised plasmas. In order to elucidate more clearly the previous results, we plot a set of initial conditions in  $Q$  versus their escape time. To do that, we consider that a trajectory escapes when it crosses the boundary of the region  $Q$  outwards and never comes back.

Fig. 8 shows the region  $Q$  in phase space which contains the set of initial conditions with the escape time in a colour bar and the respective escape time distribution for  $A_1 = 1$ ,  $A_2 = 0.1$ ,  $k_{x1} = 1$ ,  $k_{x2} = \sqrt{3}$ ,  $k_{y1} = 1$ ,  $k_{y2} = 0.5$ , and  $u = 1.5$ . In Fig. 8(a), we compute the escape times from a set of initial conditions in  $Q$  for the drift wave model with dissipation  $\mu = 10^{-3}$  and noise intensity  $\sigma = 10^{-2}$ . The white region corresponds to the initial conditions that do not escape from the phase space region and the trajectories go to some attractor. In this case without SR, the particles that go outside the region have short escape times, as shown in Fig. 8(b) by means of the escape time distribution with  $\langle \tau \rangle \approx 32$ . However, when there is SR, we can see that all initial conditions escape, and as a result the Fig. 8(c) has no white region. The escape time distribution (Fig. 8d) is skewed to the right, since a high quantity of initial conditions have an escape time larger than  $10^3$ , and the escape time is equal to  $3.3 \times 10^3$ .

#### 4. Conclusions

In the literature, a drift wave model has been used to describe particle transport in magnetised plasmas. In this work, we have studied the effect of adding noise in a model of drift waves with dissipation. Dissipation and noise can emerge from collisional effects between confined particles.

We have numerically observed that the dissipation in the noiseless two-wave model destroys the islands chains and the chaotic sea. So that as a result, the system becomes more stable than in the conservative case. The variation of the dissipation intensity produces the appearance of attractors and consequently complex basins in phase space. Moreover, we find that the escape time decreases when the dissipation parameter increases according to a power-law scale.

In the dissipative drift motion, we observe that the escape time can be maximal when the noise intensity reaches a finite level in which the phenomenon of stochastic resonance (SR) takes place. When the average escape time is small, trajectories leave the relevant domain easily, and when it is large they leave the domain slowly. The performance of the noise is its ability at becoming large the average time escape, which is an unexpected behaviour in the model considered in this work for some plasma dynamics. The noise intensity value for the SR to occur depends on the dissipation parameter, and this dependence also obeys a power-law scaling. This empirical law is still unclear to us and require further investigation. In addition, we have also observed that the escape time distribution is skewed to the right, and also the SR peak occurs earlier than all particles have escaped. Consequently, the time of confinement is improved when SR takes place in the dissipative drift motion with noise. The combination of noise and dissipation that can improve the confinement is not robust against noise outliers, due to the finite variance of the escape time as a function of the noise intensity observed in Fig. 7. Finally, we expect our work to be useful in the study of drift wave models and also for a better understanding of the SR phenomenon in different physical contexts.

## Acknowledgements

This work was possible by partial financial support from the following Brazilian government agencies: CNPq, CAPES, and Fundação Araucária. Furthermore, it has been supported by the Spanish Ministry of Economy and Competitiveness under Project No. FIS2013-40653-P and by the Spanish State Research Agency (AEI) and the European Regional Development Fund (FEDER) under Project No. FIS2016-76883-P. MAFS acknowledges the jointly sponsored financial support by the Fulbright Program and the Spanish Ministry of Education (Program No. FMECD-ST-2016).

## References

- [1] Tan WM. Microinstability theory in tokamaks. *Nucl Fusion* 1978;18.:1089–160.
- [2] Horton W. Drift waves and transport. *Rev Mod Phys* 1999;71.:735–78.
- [3] Motley RW. *Q-machines*. New York: Academic Press; 1975.
- [4] Viana RL, Da Silva EC, Kroetz T, Caldas IL, Roberto M, Sanjuán MA. Fractal structures in nonlinear plasma physics. *Phil Trans R Soc A* 2011;369.:371–95.
- [5] Hendel HW, Chu TK, Politzer PA. Collisional drift waves-identification, stabilization, and enhanced plasma transport. *Phys Fluids* 1968;11.:2426–39.
- [6] Horton W. Onset of stochasticity and the diffusion approximation in drift waves. *Plasma Phys Contr F* 1985;27.:937–56.
- [7] Marcus FA, Caldas IL, Guimarães Filho ZO, Morrison PJ, Horton W, Nascimento IC, et al. Reduction of chaotic particle transport driven by drift waves in sheared flows. *Phys Plasmas* 2008;15:112304.
- [8] Oyarzabal RS, Szezech JD, Batista AM, de Souza SL, Caldas IL, Viana RL, et al. Transient chaotic transport in dissipative drift motion. *Phys Lett A* 2016;380.:1621–6.
- [9] Planat M. Noise, oscillators and algebraic randomness: from noise in communication systems to number theory. Springer: Berlin; 2014.
- [10] Benzi R, Sutera A, Vulpiani A. The mechanism of stochastic resonance. *J Phys A* 1981;14.:453–7.
- [11] Rajasekar S, Sanjuán MAF. Nonlinear resonances. Springer Series in Synergetics: Berlin; 2015.
- [12] McDonnell MD, Abbott D. What is stochastic resonance? definitions, misconceptions, debates, and its relevance to biology. *PLoS Comput Biol* 2009;6:e1000348.
- [13] Park K, Lai Y-C. Characterization of stochastic resonance. *Europhys Lett* 2005;70.:432–8.
- [14] Gluckman BJ, Netoff TI, Neel EJ, Ditto WL, Spano ML, Schiff SJ. Stochastic resonance in a neuronal network from mammalian brain. *Phys Rev Lett* 1996;77.:4098–101.
- [15] Benzi R, Parisi G, Sutera A, Vulpiani A. Stochastic resonance in climatic change. *Tellus* 1982;34.:10–16.
- [16] Wiesenfeld K, Pierson D, Pantazelou E, Dames C, Moss F. Stochastic resonance on a circle. *Phys Rev Lett* 1994;72.:2125–9.
- [17] Liu K, Jin Y. Stochastic resonance in periodic potentials driven by colored noise. *Phys A* 2013;392.:5283–8.
- [18] Arathi S, Rajasekar S. Stochastic resonance in a single-well anharmonic oscillator with coexisting attractors. *Commun Nonlinear Sci Numer Simulat* 2014;19.:4049–56.
- [19] Schelin AB, Caldas IL, Viana RL, Benkadda S. Collisional effects in the tokamak. *Phys Lett A* 2011;376.:24–30.
- [20] Silva EC, Caldas IL, Viana RL, Sanjuán MA. Escape patterns, magnetic footprints, and homoclinic tangles due to ergodic magnetic limiters. *Phys Plasmas* 2002;9.:4917–28.
- [21] Benkadda S, Elskens Y, Ragot B. Exit times and chaotic transport in hamiltonian systems. *Phys Rev Lett* 1994;72.:2859–62.
- [22] Szezech JD, Caldas IL, Lopes SR, Viana RL, Morrison PJ. Transport properties in nontwist area-preserving maps. *Chaos* 2009;19:043108.
- [23] Szezech JD, Caldas IL, Lopes SR, Morrison PJ, Viana RL. Effective transport barriers in nontwist systems. *Phys Rev E* 2012;86:036206.
- [24] Horton W. Anomalous ion conduction from toroidal drift modes. *Plasma Phys* 1981;23.:1107–25.
- [25] Bénisti D, Escande DF. Nonstandard diffusion properties of the standard map. *Phys Rev Lett* 1998;80.:4871–4.
- [26] Elskens Y. Nonquasilinear evolution of particle velocity in incoherent waves with random amplitudes. *Commun Nonlinear Sci Numer Simulat* 2010;15.:10–15.
- [27] Batista AM, Caldas IL, Lopes SR, Viana RL, Horton W, Morrison PJ. Nonlinear three-mode interaction and drift-wave turbulence in a tokamak edge plasma. *Phys Plasmas* 2006;13:042510.
- [28] Lima GZS, Guimarães Filho ZO, Batista AM, Caldas IL, Lopes SR, Viana RL, et al. Bicoherence in electrostatic turbulence driven by high magnetohydrodynamic activity in tokamak chauffage alfvén brésilien. *Phys Plasmas* 2009;16:042508.
- [29] Horton CW, Ichikawa YH. Chaos and structures in nonlinear plasmas. Singapore: World Scientific Publishing Co Pte Ltd; 1996.
- [30] Kabantsev AA, Tsidulko YA, Driscoll CF. Chaotic neoclassical separatrix dissipation in parametric drift-wave decay. *Phys Rev Lett* 2014;112:055003.
- [31] Bernal JD, Seoane JM, Sanjuán MAF. Weakly noisy chaotic scattering. *Phys Rev E* 2013;88:032914.
- [32] Aguirre J, Viana RL, Sanjuán MAF. Fractal structures in nonlinear dynamics. *Rev Mod Phys* 2009;81.:333–86.
- [33] Seoane JM, Sanjuán MAF. New developments in classical chaotic scattering. *Rep Prog Phys* 2013;76. 16001–53.
- [34] Bianchi LA, Blömker D, Yang M. Additive noise destroys the random attractor close to bifurcation. *Nonlinearity* 2016;29:3934.
- [35] Krawiecki A, Kacperski K, Matyjaśkiewicz S, Hołyst JA. Log-periodic oscillations and noise-free stochastic multiresonance due to self-similarity of fractals. *Chaos Solitons Fractals* 2003;18.:89–96.